JCTC Journal of Chemical Theory and Computation

Article

pubs.acs.org/JCTC

Parameterization of Halogens for the Density-Functional Tight-Binding Description of Halide Hydration

Soran Jahangiri,[†] Grygoriy Dolgonos,[‡] Thomas Frauenheim,[‡] and Gilles H. Peslherbe*[,†]

[†]Centre for Research in Molecular Modeling (CERMM) and Department of Chemistry and Biochemistry, Concordia University, 7141 Sherbrooke Street West, Montréal, Québec, Canada H4B 1R6

[‡]Bremen Center for Computational Materials Science, University of Bremen, Am Fallturm 1, 28359 Bremen, Germany

Supporting Information

ABSTRACT: Parameter sets of the self-consistent-charge density-functional tight-binding model with and without its third-order extension have been developed to describe the interatomic interactions of halogen elements (X = Cl, Br, I) with hydrogen and oxygen, with the ultimate goal of investigating halide hydration with this approach. The reliability and accuracy of the model with these newly developed parameters has been evaluated by comparing the structural, energetic, and vibrational properties of small molecules containing halogen atoms with those obtained by means of standard density-functional theory. Furthermore, the newly parametrized model is found to predict equilibrium geometries, binding energies, and vibrational frequencies for small aqueous clusters containing halogen anions, $X^-(H_2O)_n$ (n = 1−4), in good agreement with those calculated with density-functional theory and high-level ab initio quantum chemistry and with available experimental data. This demonstrates that the newly parametrized models might be a method of choice for investigating halide hydration in larger clusters.

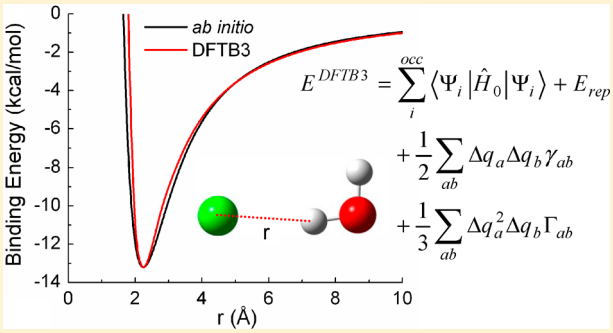

1. INTRODUCTION

The hydration of ions has been the subject of extensive investigations in recent years.[1−5] In particular, the propensity of large and polarizable anions to locate toward air−water interfaces has garnered increasing attention and a variety of experimental and theoretical studies have shown unambiguously a systematic increase of the surface concentration of such soft anions.[6−10] These observations can be used to provide evidence for the molecular determinants of the behavior of solvated ions such as the specific ion effect.[11,12] This warrants a comprehensive molecular-level understanding of the underlying mechanisms that govern ion solvation.

Halogen anions, i.e. halides, have long been a paradigm for investigating the behavior of solvated ions,[13−20] as the effects of size, charge density, and polarizability on the ion solvation structures, the ion−solvent interactions, and the spectroscopic signature of hydrogen bonding can be investigated comparatively across the halide series. The presence of halides in atmospheric droplets or clouds over the marine boundary layer has also motivated a large body of experimental and theoretical investigations.[2,7,9] In this respect, electronic structure theory methods can be used to investigate ion−solvent interactions through accurate evaluation of structural, energetic, and spectroscopic properties of halide-containing water clusters. However, application of these methods, and in particular the high-level electron correlation ones, is restricted to small systems because of high computational cost. As an alternative, semiempirical and approximate methods with affordable computational costs could be used to overcome this deficiency and to facilitate electronic structure calculations for larger systems. Accordingly, the development and validation of practical approximate methods are essential to extend the applicability of theoretical investigations to larger systems.

The density-functional tight-binding (DFTB) model[21] is an approximate method based on density-functional theory (DFT) and the tight-binding method with a computational cost up to 3 orders of magnitude lower than that of conventional DFT.[22] Therefore, the efficiency of the DFTB model makes it an appropriate approach for investigating systems for which DFT and ab initio quantum chemistry calculations are prohibitively time-consuming. Similarly to semiempirical molecular orbital methods, this efficiency is achieved by considering explicitly only the valence electrons in the system and by evaluating Hamiltonian and overlap matrix elements as predetermined parametrized quantities. But in contrast to most semiempirical methods, matrix elements are not considered as adjustable parameters and are evaluated directly from reference DFT calculations for each pair of atoms as a function of interatomic distance. The main advantage of this approach lies in the generation of parameters that are not dependent on reference systems used as a basis for parametrization and are presumably more transferable. It has been shown that for systems containing atoms with different electronegativities the accuracy

Received: October 23, 2012
Published: June 26, 2013

of the DFTB model is significantly improved by adjusting atomic charge distributions through adding a self-consistent-charge term to the DFTB energy.[23] DFTB and its self-consistent-charge version (often referred to as DFTB2) have been successfully applied to various systems and the validity of the model in predicting structural and energetic properties as well as vibrational frequencies has been previously demonstrated.[24−32] Moreover, DFTB2 has been further extended to a model known as DFTB3 that even better describes systems containing charged species.[33,34]

In this work, DFTB2 and DFTB3 parameters have been generated for the description of H−X and O−X (X = Cl, Br, I) interactions, following a procedure that has revealed highly successful before for systems containing organic and biological molecules,[23,33−35] zinc,[36] titanium,[37] cadmium, selenium, tellurium,[38] and boron,[39] among other works of similar scope. The accuracy of the newly parametrized model has been validated for selected systems and properties against results of DFT and ab initio quantum chemistry calculations. Particular attention was paid to the equilibrium geometries, atomization energies, and harmonic vibrational frequencies of hydrogen halides and halogen oxoacids, as well as the geometries, binding energies, and vibrational frequencies of halide-containing water clusters. The outline of this article is as follows: the computational methodology and the details of the parametrization are given in section 2, the results obtained with the newly parametrized model for halogen-containing molecules and halide−water clusters are presented and discussed in section 3, and concluding remarks follow in section 4.

2. COMPUTATIONAL METHODOLOGY

2.1. DFTB Models. The expansion of the DFT energy in terms of charge density fluctuations over a reference electron density is the basic framework of various DFTB models. The reference density is chosen as the localized (or compressed) electron density of neutral atoms in order to mimic the behavior of interacting atoms in molecular (or periodic) systems, for which atomic densities expand to a lesser extent than for isolated atoms. On the basis of this framework, the standard DFTB energy is obtained from a zeroth-order expansion as follows:[24]

$$E^{\mathrm{DFTB0}} = \sum_{i}^{\mathrm{occ}} \langle \Psi_i | \hat{H}_0 | \Psi_i \rangle + E_{\mathrm{rep}} \tag{1}$$

where the first term is the so-called band-structure energy, which is the sum over one-electron orbital energies given a reference Kohn−Sham Hamiltonian $\hat{H}_0$, and the second term represents the repulsion energy. The DFTB2 energy is constructed by expanding the DFT energy up to second-order, which amounts to adding a self-consistent charge correction:[23]

$$\begin{aligned} E^{\mathrm{DFTB2}} &= E^{\mathrm{DFTB0}} + E^{\mathrm{2nd\text{-}order}} \\ &= E^{\mathrm{DFTB0}} + \frac{1}{2}\sum_{ab} \Delta q_a \Delta q_b \gamma_{ab} \end{aligned} \tag{2}$$

where Δq_a and Δq_b are induced atomic charges derived from Mulliken charges that are solved for self-consistently and γ_{ab} is a function of chemical hardness. The DFTB3 model is obtained by including a third-order term to the energy expansion:[33]

$$\begin{aligned} E^{\mathrm{DFTB3}} &= E^{\mathrm{DFTB2}} + E^{\mathrm{3rd\text{-}order}} \\ &= E^{\mathrm{DFTB2}} + \frac{1}{3}\sum_{ab} \Delta q_a{}^2 \Delta q_b \Gamma_{ab} \end{aligned} \tag{3}$$

where Γ_{ab} represents the change of γ_{ab} with respect to charge.

The one-electron orbital energies in eq 1 are obtained by solving Kohn−Sham equations ($\hat{H}_0\Psi_i = \varepsilon_i\Psi_i$) in which each orbital Ψ_i is represented as a linear combination of pseudoatomic Slater-type basis functions initially optimized from DFT calculations using an effective potential augmented by a harmonic term of the form $(r/r_0)^n$ to compress the orbitals on the nucleus.[21,23] The exponent n is usually chosen as 2, and the radius r_0 is taken as twice the covalent radius (r_c) for all atom types.[40] Along with the optimized exponents of the Slater-type functions, such DFT calculations also provide reference atomic electron densities, which are used in the effective potential of the Hamiltonian $\hat{H}_0$, making the Kohn−Sham equations no longer iterative in the DFTB model (but not in the DFTB2 and DFTB3 versions since the Hamiltonian is modified to account for the induced charges). The Hamiltonian and overlap matrix integrals in the localized atomic basis are evaluated as a function of interatomic distance for each pair of atom types, and the Slater-Koster formalism[41] allows one to restrict their evaluation to a limited number of specific orientations of atomic orbitals. Such calculations are performed once, and the resulting values are tabulated so that these quantities can be simply evaluated by interpolation of the tabulated data in future calculations.

The repulsion term is represented as a sum over pairwise, short-range, diatomic repulsion potentials.[24] These potentials are calculated as a function of interatomic distance by subtracting the electronic DFTB energy from the DFT energy for any type of atom pair. Similarly to the Hamiltonian and overlap matrix elements, reference diatomic repulsion potentials are evaluated once and tabulated for future calculations.[42] The evaluation of repulsion potentials from DFT calculations compensates (at least in part) for the errors due to the approximations made in evaluating the DFTB electronic energies.

As mentioned earlier, the second-order term in eq 2 is obtained from the calculation of Mulliken atomic charges of two interacting atoms in a self-consistent manner. The γ_{ab} function in eq 2 represents the extent of charge interaction as a function of distance and can be formulated by assuming the following two limits.[23,33] At long distances, the charge interaction can be considered as a Coulomb interaction between two separated point charges, which makes the γ_{ab} function simply the inverse of the distance between the charges. At zero distance, the γ_{ab} function represents the self-interaction and can be approximately related to the second-order derivative of the energy with respect to the occupation number of the highest occupied atomic orbital, the so-called Hubbard parameter, which is related to the ionization potential and the electron affinity. On the basis of these two limits, and assuming an exponential decay for charge densities, an analytical expression has been obtained for γ_{ab} as a function of interatomic distance, which depends on the Hubbard parameter of each atom.[23] The values of the Hubbard parameters can be calculated by DFT for each atom type and tabulated together with the matrix elements and diatomic repulsion potentials. It should be noted that inclusion of a

modified γ_{ab} function for H−X interactions (γ^h) leads to a better description of hydrogen bond energies.[43,44]

In DFTB3, the dependence of the γ_{ab} function on atomic charges is also taken into account by introducing the Γ_{ab} function, $\Gamma_{ab} = \partial\gamma_{ab}/\partial q_a|_{q_a^0}$.[33] The latter can be obtained from the chain rule as the product of the derivative of the γ_{ab} function with respect to the Hubbard parameter ($\partial\gamma_{ab}/\partial U_a$) and the derivative of the Hubbard parameter with respect to charge ($\partial U_a/\partial q_a|_{q_a^0}$). The former term is obtained analytically and the latter one, which represents the third-order derivative of the total atomic energy with respect to charge, is calculated from the values of the Hubbard parameter obtained in different charged states.[33] Inclusion of the third-order energy term allows a better treatment of systems containing negatively charged ions.[33,34]

In summary, the parametrization of DFTB involves calculating and tabulating the reference matrix elements and pairwise repulsion terms as a function of interatomic distance for any desired pair of atom types. In this way, the DFTB model is solely parametrized on the basis of DFT data without including any adjustable empirical parameter.

2.2. Computational Details. Reference electron densities and pseudoatomic wave functions have been obtained by solving atomic Kohn−Sham equations with the Perdew, Burke, and Ernzerhof (PBE)[45] exchange-correlation functional. As mentioned earlier, the effective potential also includes a $(r/r_0)^2$ term where the choice of r_0 is based on the covalent radius of each atom type. In this work, two different values of r_0 were used for generating reference densities and optimizing basis functions, in agreement with the procedure previously implemented to obtain the *parameters for materials and biological systems (MIO)*[23] and *DFTB3 parameters for organic and biological applications (3OB)*.[34] The oxygen and hydrogen radii were chosen as those used to generate the MIO and 3OB parameters, and analogous criteria were employed for generating the halogen radii. However, the latter were slightly adjusted to better reproduce the energy gap between the highest occupied and the lowest unoccupied atomic orbitals predicted by DFT calculations with the hybrid exchange-correlation functional of PBE and Adamo.[45,46] The resulting r_0 values for halogen atoms are $8r_c$ and $1.5r_c$ for generating the reference densities and optimizing the basis functions, respectively, which are within the range employed in earlier works.[39] It should be noted that the choice of the confinement radii does not have a significant influence on the resulting molecular properties, as pointed out in earlier investigations.[40] The Hamiltonian and overlap matrix elements have been obtained by considering an s orbital for hydrogen, s and p orbitals for oxygen and s, p, and d orbitals for halogen atoms. The diagonal elements of the Hamiltonian matrix are the eigenvalues of the Hamiltonians for the free atoms, and the off-diagonal elements are obtained from a two-center approximation.[23] The Hubbard derivatives were found to be −0.06, −0.05, and −0.04 au for chlorine, bromine, and iodine, respectively, and the adjustable parameter of the γ^h function was set to 4.0 for consistency with the 3OB set.[34]

Pairwise repulsion potentials have been obtained on the basis of DFT results obtained with the Becke 3-parameter Lee−Yang−Parr (B3LYP)[47−49] functional for X_2, HX, and HOX molecules as reference systems for characterizing X−X, H−X, and O−X interactions (X = Cl, Br, I), respectively. The DFTB2 parametrization was performed on the basis of all-electron basis set reference data obtained with the 6-31G(d) basis set for molecules containing chlorine[50]- and bromine[51] and the 6-311G(d) basis set for molecules containing iodine[52−54] to keep the parameters consistent with the MIO[23] set developed, previously. A larger basis set was found to be necessary to describe the highly polarizable iodine. The DFTB3 parameters were obtained on the basis of reference data obtained with the cc-pVTZ[55] basis set for consistency with the 3OB[34] set developed more recently. For systems containing bromine and iodine, effective core potentials (cc-pVTZ-PP basis set)[53,54,56,57] were used to partially include relativistic effects. However, it should be noted that previous investigations[58,59] of heavier halide hydration have employed all-electron basis set methods, since relativistic effects appear unimportant for these systems.

In order to predict accurate bond dissociation energies, the resulting repulsion curves have been adjusted by shifting them up to reproduce the DFT bond dissociation energies for the reference systems.[37] The shifted curves were then exponentially extended to zero. For H−X interactions, instead of using such exponentially decaying functions, repulsion curves were connected to the tail of the curve obtained for the $X^-(H_2O)$ system. A similar procedure was originally employed for carbon−carbon interactions where different molecules with different bond orders were used to generate different regions of the carbon−carbon repulsion curve.[40]

All PBE calculations used to generate the reference electron densities and optimizing the basis functions, as well as generating Hamiltonian and overlap matrix elements, were performed with an in-house code called Twocnt. The DFTB+ code[60] was used for DFTB calculations, while all DFT and ab initio quantum chemistry calculations were performed using the Gaussian09 suite of programs.[61] The conjugate-gradient method (with a force threshold of 10^{-5} au) was used for DFTB geometry optimizations, and all necessary parameters for hydrogen and oxygen were taken from the MIO[23] and 3OB[34] sets. Atomization energies (AEs) were calculated for halogen-containing molecules as the difference between the energy of the molecule and the sum of those of its dissociated atoms. All values were corrected for zero-point energy. The reference halogen, oxygen, and hydrogen atoms were considered as spin-polarized systems in DFTB calculations[62] (the respective spin constants for halogen atoms are listed in Table S1 of the Supporting Information) and the corresponding DFT calculations were performed within the unrestricted-spin formalism (UB3LYP). All ab initio quantum chemistry calculations for halide−water clusters were performed with frozen-core second-order Møller−Plesset (MP2) theory[63] using Dunning's correlation-consistent aug-cc-pVTZ basis set for chlorine[55] and the aug-cc-pVTZ-PP basis set for bromine[56] and iodine.[53,54,57] Stepwise binding energies of halide−water clusters were calculated as follows:

$$\Delta E_{n,n-1} = E[X^-(H_2O)_n] - E[X^-(H_2O)_{n-1}] - E[H_2O] \quad (4)$$

where $E[\ ]$ denotes the total energy of the species in brackets. All DFT and ab initio cluster binding energies were further corrected for basis set superposition error (BSSE) using the counterpoise procedure of Boys and Bernardi.[64] We note that such corrections can not be properly implemented in DFTB calculations, which employ predetermined matrix elements to calculate energies. However, since the model employs a minimal basis set of localized function to construct the molecular wave function, DFTB is not expected to suffer

from BSSE. Moreover, inclusion of a modified γ_{ab} function with an empirical adjustable parameter for hydrogen-bonded systems might also partially compensate for BSSE in evaluating cluster binding energies.

3. RESULTS AND DISCUSSION

In order to validate the accuracy of the newly generated DFTB parameters and benchmark their reliability for investigating halide hydration, structural, energetic, and vibrational properties have been calculated for small covalent molecules containing halogen atoms and water clusters containing halides, and the results have been compared with those predicted by DFT and with available experimental data. Cluster properties have also been compared with the results of high-level MP2 calculations. In the following, the discussion will focus primarily on DFTB3 results, with reference to DFTB2 results occasionally for comparison.

3.1. Covalent Systems. A test set of 18 molecules, namely X_2, HX, and HXO_{1-4} (X = Cl, Br, I), has been examined. The structures of the molecules are shown in Figure 1, while selected geometrical and energetic properties are collected in Tables 1−3 for each molecule, and all molecular vibrational frequencies (reported in more detail as Supporting Information in Tables S2−S4) are compared in Figure 2.

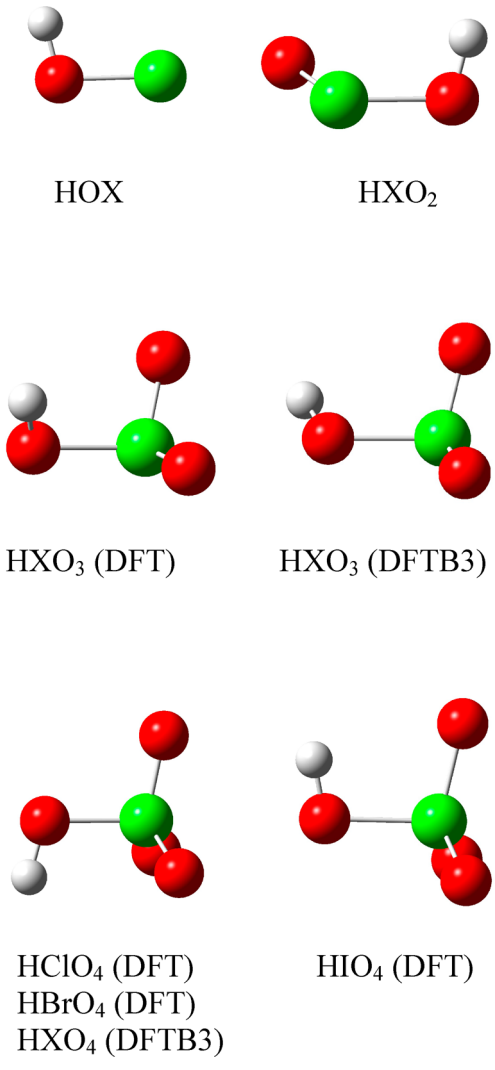

Figure 1. Optimized structures of HXO_{1-4} (X = Cl, Br, I) molecules.

3.1.1. Chlorine-Containing Molecules. All optimized DFTB3 molecular geometries for chlorine-containing molecules coincide with their DFT counterparts (cf. Figure 1), with the exception of $HClO_3$ which exhibits some slight differences. The DFTB3 energy difference between the $HClO_3$ DFT-optimized structure and the global-minimum-energy structure is only 3.8 kcal/mol, which is negligible in light of the energetics discussed below. Inspection of Table 1 indicates that DFTB3 bond lengths are accurately predicted compared to DFT and experimental values. Generally, DFTB3 Cl—O single-bond lengths are larger than their DFT counterparts (with a maximum absolute deviation of 0.053 Å obtained for $HClO_3$), whereas DFTB3 Cl═O double-bond lengths are usually smaller than their DFT counterparts (by no more than 0.02 Å). Similarly, calculated Cl—O—H bond angles are also overestimated by DFTB3, with an average deviation of about 7−9° from reference DFT and experimental values.

As for the energetics of bond breaking, DFTB3 reproduces the Cl_2, HCl, and HOCl AEs predicted by DFT, which are underestimated relative to experimental data. This is not surprising, since this DFT data is the basis for the parametrization of DFTB3. In the larger $HClO_{3-4}$ molecules, the deviations of the AEs increase by about 20 kcal/mol per additional Cl═O bond, most likely reflecting the fact that the chlorine-oxygen DFTB3 repulsion profile was mostly parametrized on the basis of Cl−O single-bond data and, as a result, Cl═O double bonds are described less accurately by the model.

Harmonic vibrational frequencies, as they reflect the curvature of the potential energy surface (PES) around the equilibrium geometry, are typically more sensitive to the description of interatomic interactions than the molecular geometry or the energy itself. In general, when compared to DFT values, the frequencies of the Cl—Cl and Cl—H bond stretching modes are accurately predicted by DFTB3 whereas those of the Cl—O and Cl═O stretching modes tend to be moderately underestimated, especially for the larger $HClO_{3-4}$ molecules (cf. Supporting Information Table S2). The calculated DFTB3 frequencies correlate well with the DFT values, as shown in Figure 2; with the exception of a very few outliers, DFTB3 underestimates frequencies by ca. 10% on average.

3.1.2. Bromine-Containing Molecules. Similar to chlorine-containing systems, molecular shapes of optimized DFTB3 structures of bromine-containing molecules agree well with those from DFT (cf. Figure 1), except for $HBrO_3$, for which the H atom rotates around the Br−O bond. DFTB3 predicts an asymmetric structure for $HBrO_3$ which differs from the DFT-optimized structure by 5.9 kcal/mol. Similar to the chlorine case, DFTB3 bond lengths are in good agreement with DFT and experimental values in most cases (cf. Table 2). DFTB3 maximum absolute deviations for Br—O and Br═O bond lengths are 0.066 and 0.068 Å (observed for $HBrO_4$ and $HBrO_2$), respectively. DFTB3 bond angles are overestimated by about 9° relative to DFT and experimental values, which is comparable to the deviations observed for chlorine-containing compounds.

The DFTB3 AEs of Br_2, HBr, and HOBr are in a good agreement with DFT and experimental values. As for the $HBrO_{2-4}$ molecules, DFTB3 predicts AEs that are increasingly overestimated, presumably because of the growing number of

dx.doi.org/10.1021/ct300919h | J. Chem. Theory Comput. 2013, 9, 3321−3332

Table 1. Selected Geometric and Energetic Properties of Various Chlorine Compounds

molecule		DFTB3	DFT[a]	exp
bond length (Å)				
Cl_2	Cl—Cl	2.025	2.024	1.988[b]
HCl	Cl—H	1.278	1.283	1.275[b]
HOCl	Cl—O	1.711	1.710	1.689[c]
$HClO_2$	Cl—O	1.723	1.730	
	Cl═O	1.504	1.524	
$HClO_3$	Cl—O	1.790	1.737	
	Cl═O	1.450, 1.463	1.459, 1.467	
$HClO_4$	Cl—O	1.730	1.684	1.64[d]
	Cl═O	1.437, 1.451 (2)	1.430, 1.440 (2)	1.404, 1.414 (2)[d]
Δ (DFT)[e]		0.9		
Δ (exp)		2.3	1.7	
bond angle (deg)				
HOCl	Cl—O—H	109.8	102.8	103.1[c]
$HClO_2$	Cl—O—H	112.5	103.9	
$HClO_3$	Cl—O—H	112.3	103.0	
$HClO_4$	Cl—O—H	114.0	104.7	
Δ (DFT)		8.2		
Δ (exp)		6.5	0.3	
AE (kcal/mol)				
Cl_2		53.1	53.1	57.2[f]
HCl		100.0	100.1	102.2[f]
HOCl		150.5	152.9	156.3[f]
$HClO_2$		202.2	181.9	
$HClO_3$		279.7	235.7	
$HClO_4$		346.4	277.0	
Δ (DFT)		9.4		
Δ (exp)		4.3	3.8	

[a]B3LYP/cc-pVTZ. [b]From ref 67. [c]From ref 68. [d]From ref 69. [e]Δ is the absolute mean deviation of DFTB3 data from reference data in parentheses (%). [f]From ref 70.

Br═O bonds poorly described by the model, as was observed for analogous chlorine-containing molecules.

The DFTB3 frequencies of the Br—Br and Br—H vibrations are underestimated relative to DFT values (Supporting Information Table S3), with deviations larger than those observed in the corresponding chlorine-containing molecules, but the magnitude of the deviations in the Br—O and Br═O stretching and bending frequencies are comparable to their counterparts for $HClO_{1-4}$ molecules in most cases. In general, DFTB3 frequencies correlate well with DFT values, as shown in Figure 2. Overall the average deviation of DFTB3 frequencies is about 10% after exclusion of a few outliers.

3.1.3. Iodine-Containing Molecules. The DFTB3 optimized geometries of iodine-containing molecules follow the same trend in molecular shapes that has been observed in the case of bromine-containing molecules, including the differences in the optimized HIO_3 structure with the DFT one due to rotation of the O—H bond around the single iodine−oxygen bond (cf. Figure 1). DFTB3 predicts a HIO_3 structure which differs in energy by 3.8 kcal/mol from the DFT-optimized one. DFTB3 also predicts the HIO_4 DFT-optimized structure to be a transition state with an imaginary frequency of 167i cm^{-1}, lying only 0.2 kcal/mol above the minimum. This finding indicates that the DFTB3 PES is relatively flat along the direction toward the minimum-energy structure. The DFTB3 bond lengths and angles of iodine-containing molecules are also in good agreement with the reference data (cf. Table 3). The maximum absolute deviation relative to DFT is 0.084 Å for I—O, while the maximum deviation for I═O is only 0.029 Å, both in HIO_4. Deviations in bond angles within 7° are observed, relative to DFT and experimental data, which are smaller than those observed for chlorine- and bromine-containing molecules.

The DFTB3 AEs for I_2, HI, and HOI are in good agreement with DFT values. For larger HIO_{2-4} molecules, deviations in the AE of about 6−10 kcal/mol are observed upon addition of I═O bonds, which are less than those observed for chlorine- and bromine-containing molecules.

DFTB3 underestimates the frequency of the I—I and I—H stretching modes relative to DFT and experimental values (Supporting Information Table S4). The frequencies of the I—O and I═O stretching modes are mostly underestimated by DFTB3 relative to DFT values, with deviations increasing in larger molecules. However, the I—O stretching frequencies are better reproduced by DFTB3, compared to the Cl—O ones. As depicted in Figure 2, a fairly good correlation was found between the DFTB3 harmonic frequencies of the iodine systems under consideration and those from DFT. Overall, the average deviation of DFTB3 frequencies is about 10% with respect to reference DFT values with the exception of a few points.

3.2. Halide−Water Clusters. Halide−water clusters containing each of the halides and up to four water molecules have been considered as a test set. All the minimum-energy cluster structures predicted by ab initio quantum chemistry and shown in Figure 3 are correctly reproduced by DFTB3 (and all have the same geometrical arrangement of water molecules around the ion regardless of the halide). DFTB3 reference hydrogen-bond lengths and angles are presented in Tables 4−6,

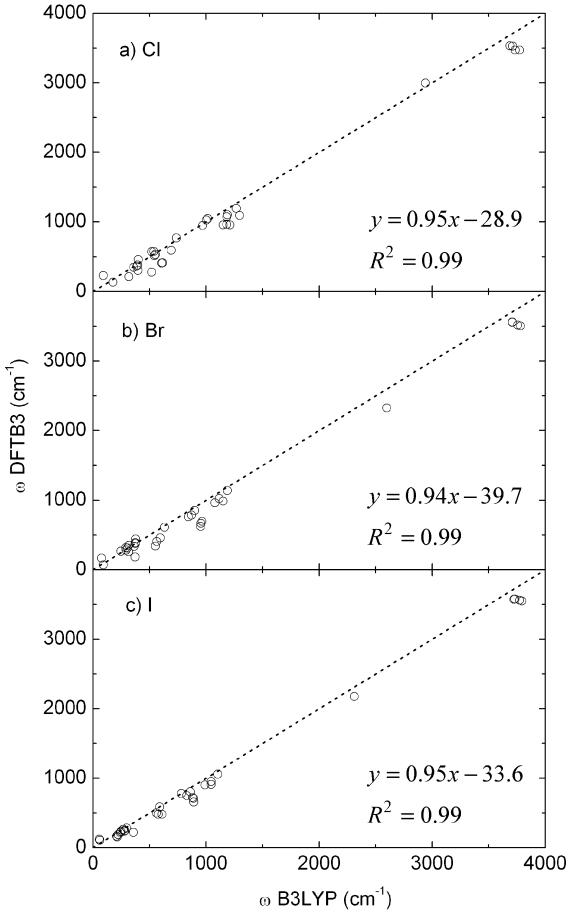

Figure 2. Calculated harmonic vibrational frequencies for halogen-containing compounds.

Table 2. Selected Geometric and Energetic Properties of Various Bromine Compounds

molecule		DFTB3	DFT[a]	exp
bond length (Å)				
Br_2	Br—Br	2.335	2.316	2.281[b]
HBr	Br—H	1.423	1.425	1.414[b]
HOBr	Br—O	1.830	1.846	1.834[c]
$HBrO_2$	Br—O	1.860	1.859	
	Br═O	1.600	1.668	
$HBrO_3$	Br—O	1.890	1.847	
	Br═O	1.551, 1.569	1.616, 1.620	
$HBrO_4$	Br—O	1.873	1.807	
	Br═O	1.533, 1.551 (2)	1.597, 1.605 (2)	
Δ (DFT)[d]		2.4		
Δ (exp)		1.1	1.0	
bond angle (deg)				
HOBr	Br—O—H	111.0	103.1	102.3[c]
$HBrO_2$	Br—O—H	113.8	104.8	
$HBrO_3$	Br—O—H	114.6	104.9	
$HBrO_4$	Br—O—H	115.4	105.6	
Δ (DFT)		8.7		
Δ (exp)		8.5	0.8	
AE (kcal/mol)				
Br_2		48.5	47.9	45.5[e]
HBr		87.6	87.2	86.6[e]
HOBr		148.3	150.6	150.2[e]
$HBrO_2$		205.5	183.1	
$HBrO_3$		282.5	238.2	
$HBrO_4$		340.0	266.1	
Δ (DFT)		10.3		
Δ (exp)		3.0	2.1	

[a]B3LYP/cc-pVTZ-PP. [b]From ref 67. [c]From ref 71. [d]Δ is the absolute mean deviation of DFTB3 data from reference data in parentheses (%). [e]From ref 70.

stepwise binding energies are plotted in Figure 4, ion−water potential energy curves are compared in Figure 5, selected harmonic vibrational frequencies are presented in Table 7, and all frequencies are compared to reference data in Figure 6, while atomic partial charges are presented in Table 8.

3.2.1. Chloride−Water Clusters. The results of Table 4 indicate that DFTB3 underestimates bond lengths in all cases, with average deviations of 0.103 and 0.044 Å relative to DFT and ab initio values, respectively. Bond angles are in better agreement with DFT values, with deviations of about 7°, but are underestimated by about 11° compared to ab initio ones. These observations are in accord with the general tendency of DFTB models to predict short hydrogen bond lengths,[40] which has also been observed for other types of water clusters.[33,65]

DFTB3 stepwise cluster binding energies are in good agreement with reference data with average deviations of 1.1 and 0.3 kcal/mol relative to DFT and to ab initio values, respectively, and are consistent with similar data for singly charged anion−water clusters.[65] Interestingly, DFTB3 binding energies reproduce the trend of ab initio data better than that predicted by DFT (cf. Figure 4), presumably due to the good agreement between DFTB3 and ab initio Cl···H bond lengths, while DFT tends to overestimate Cl···H bond lengths relative to ab initio values. As for binding energies, the DFTB2 model underestimates the ab initio values by about 2 kcal/mol. The improvement in the energetics in DFTB3 model might be due to the better performance of this model in describing interatomic charge transfer, as shown from the data in Table 8, where charge distributions are seen to converge toward ab initio ones sequentially as one turns on the hydrogen bond and third-order corrections. The chloride−water potential energy curve shown in Figure 5a further reflects the good agreement between DFTB3 and ab initio energetics.

As shown in Figure 3, the global minimum structure in $Cl^-(H_2O)_1$ is asymmetric with only one semilinear hydrogen bond. This asymmetric structure, which has been confirmed experimentally,[66] is correctly reproduced by DFTB3. Results in Table 7 indicate that the DFTB3 frequency of the free O−H stretch lies almost halfway between the reference data (DFT and ab initio) and the experimental one with DFT overestimating it by 151 cm^{-1} relative to the experimental value. DFTB3 predicts lower harmonic frequencies of the hydrogen-bonded O−H stretch—by 417 and 224 cm^{-1} relative to DFT and experimental values, respectively. On the other hand, the red shift of the frequency of the water O−H stretch upon forming a hydrogen bond with chloride becomes too large with DFTB3—by 336 and 294 cm^{-1}, compared to DFT and experimental data, respectively. In addition, DFTB3 better reproduces lower frequencies relative to DFT, ab initio and experimental values. Overall, the average deviation of the DFTB3 frequencies from experimental data is comparable to that predicted by ab initio quantum chemistry for this cluster size.

In $Cl^-(H_2O)_2$, the two water molecules form a single hydrogen bond with chloride and another hydrogen bond with

Table 3. Selected Geometric and Energetic Properties of Various Iodine Compounds

molecule		DFTB3	DFT[a]	exp
bond length (Å)				
I_2	I—I	2.698	2.702	2.666[b]
HI	I—H	1.624	1.621	1.609[b]
HOI	I—O	2.020	2.015	1.987[c]
HIO_2	I—O	2.036	2.001	
	I═O	1.840	1.835	
HIO_3	I—O	2.042	1.974	
	I═O	1.808, 1.818	1.789, 1.790	
HIO_4	I—O	2.026	1.942	
	I═O	1.795, 1.808 (2)	1.779 (2), 1.785	
Δ (DFT)[d]		1.4		
Δ (exp)		1.3	1.2	
bond angle (deg)				
HOI	I—O—H	111.0	104.4	103.9[c]
HIO_2	I—O—H	113.9	106.9	
HIO_3	I—O—H	114.5	108.3	
HIO_4	I—O—H	115.9	106.9	
Δ (DFT)		6.8		
Δ (exp)		6.8	0.5	
AE (kcal/mol)				
I_2		42.8	42.7	35.6[e]
HI		74.8	74.6	70.4[e]
HOI		148.0	150.4	
HIO_2		200.5	191.0	
HIO_3		268.3	257.0	
HIO_4		316.2	290.5	
Δ (DFT)		3.4		
Δ (exp)		13.2	13.0	

[a]B3LYP/cc-pVTZ-PP. [b]From ref 67. [c]From ref 72. [d]Δ is the absolute mean deviation of DFTB3 data from reference data in parentheses (%). [e]From ref 70.

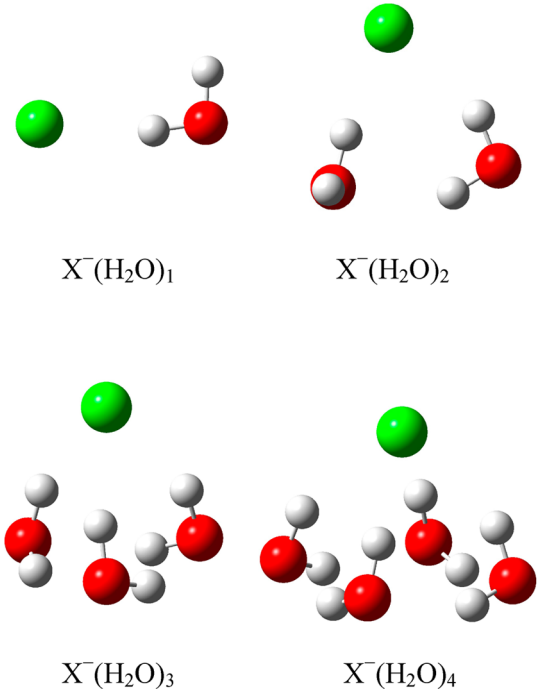

Figure 3. Optimized structures of $X^-(H_2O)_{1-4}$ clusters (X = Cl, Br, I).

Table 4. Hydrogen-Bonding Geometrical Characteristics of Chloride−Water Clusters

cluster	DFTB3	DFT[a]	ab initio[b]
bond length (Å)			
$Cl^-(H_2O)_1$	2.057	2.160	2.116
$Cl^-(H_2O)_2$	2.033	2.141	2.097
	2.303	2.365	2.294
$Cl^-(H_2O)_3$	2.218	2.332	2.266
$Cl^-(H_2O)_4$	2.296	2.423	2.335
Δ (DFT)[c]	4.5		
Δ (ab initio)	2.0	2.8	
bond angle (deg)			
$Cl^-(H_2O)_1$	156.9	164.5	168.8
$Cl^-(H_2O)_2$	156.0	163.2	168.0
	145.6	153.6	156.1
$Cl^-(H_2O)_3$	145.0	152.0	154.4
$Cl^-(H_2O)_4$	141.0	148.6	151.7
Δ (DFT)	4.8		
Δ (ab initio)	6.8	2.1	

[a]B3LYP/cc-pVTZ. [b]MP2/aug-cc-pVTZ. [c]Δ is the absolute mean deviation of DFTB3 data from reference data in parentheses (%).

Table 5. Hydrogen-Bonding Geometrical Characteristics of Bromide−Water Clusters

cluster	DFTB3	DFT[a]	ab initio[b]
bond length (Å)			
$Br^-(H_2O)_1$	2.280	2.374	2.293
$Br^-(H_2O)_2$	2.241	2.336	2.261
	2.485	2.612	2.463
$Br^-(H_2O)_3$	2.405	2.536	2.423
$Br^-(H_2O)_4$	2.471	2.625	2.479
Δ (DFT)[c]	4.8		
Δ (ab initio)	0.7	4.7	
bond angle (deg)			
$Br^-(H_2O)_1$	154.2	160.9	167.5
$Br^-(H_2O)_2$	154.0	160.3	166.5
	146.7	150.9	155.1
$Br^-(H_2O)_3$	144.8	150.2	152.8
$Br^-(H_2O)_4$	140.8	146.5	150.6
Δ (DFT)	3.7		
Δ (ab initio)	6.5	3.0	

[a]B3LYP/cc-pVTZ-PP. [b]MP2/aug-cc-pVTZ-PP. [c]Δ is the absolute mean deviation of DFTB3 data from reference data in parentheses (%).

each other. The DFTB3 frequencies for both hydrogen-bonded O−H stretching modes are smaller than for their DFT and experimental counterparts but are in better agreement with experimental data than with DFT values. As observed in the case of $Cl^-(H_2O)$, DFTB3 also overestimates the magnitude of the frequency red shift for the O−H stretches upon hydrogen bonding by 337 and 315 cm^{-1} with respect to DFT and experimental data, respectively. Interestingly, the average deviation of DFTB3 frequencies from available experimental data is smaller than that predicted by DFT and ab initio quantum chemistry, presumably due to a fortunate cancellation of errors.

In $Cl^-(H_2O)_{3-4}$, all water molecules form a single hydrogen bond with chloride ion and hydrogen bonds with neighboring water molecules to form a ring below the ion. For these larger clusters, a few vibrational modes become strongly coupled and

dx.doi.org/10.1021/ct300919h | J. Chem. Theory Comput. 2013, 9, 3321−3332

Table 6. Hydrogen-Bonding Geometrical Characteristics of Iodide−Water Clusters

cluster	DFTB3	DFT[a]	ab initio[b]
bond length (Å)			
$I^-(H_2O)_1$	2.518	2.675	2.559
$I^-(H_2O)_2$	2.437	2.613	2.508
	2.761	2.950	2.745
$I^-(H_2O)_3$	2.612	2.827	2.673
$I^-(H_2O)_4$	2.690	2.931	2.733
Δ (DFT)[c]	7.0		
Δ (ab initio)	1.8	5.8	
bond angle (deg)			
$I^-(H_2O)_1$	148.2	156.8	164.4
$I^-(H_2O)_2$	150.3	156.1	164.2
	143.5	147.7	152.9
$I^-(H_2O)_3$	142.7	147.2	151.6
$I^-(H_2O)_4$	137.8	145.2	147.9
Δ (DFT)	4.0		
Δ (ab initio)	7.4	3.5	

[a]B3LYP/cc-pVTZ-PP. [b]MP2/aug-cc-pVTZ-PP. [c]Δ is the absolute mean deviation of DFTB3 data from reference data in parentheses (%).

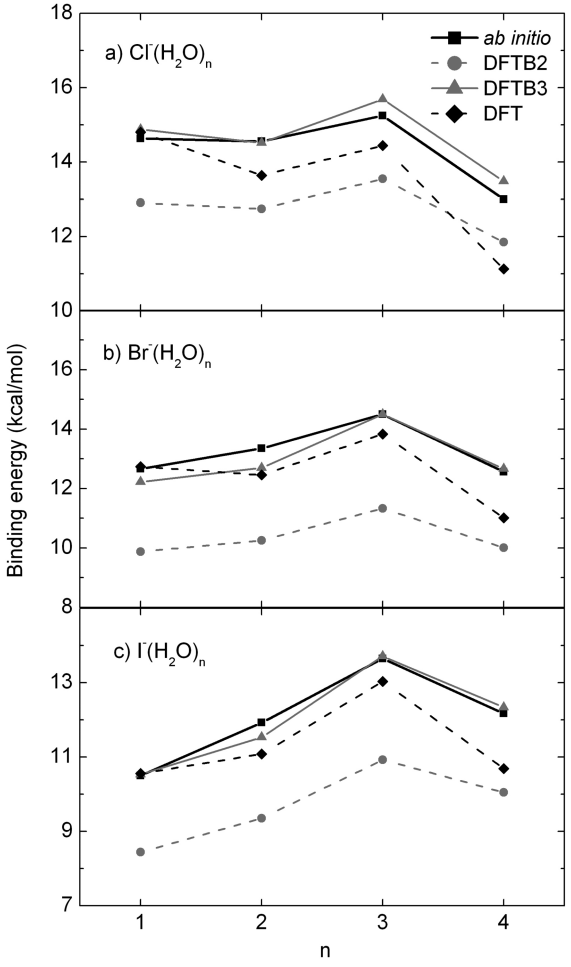

Figure 4. Stepwise binding energies of $X^-(H_2O)_n$ clusters (X = Cl, Br, I): ab initio = MP2/aug-cc-pVTZ for $Cl^-(H_2O)_{1-4}$ and MP2/aug-cc-pVTZ-PP for $Br^-(H_2O)_{1-4}$ and $I^-(H_2O)_{1-4}$; DFT = B3LYP/cc-pVTZ for $Cl^-(H_2O)_{1-4}$ and B3LYP/cc-pVTZ-PP for $Br^-(H_2O)_{1-4}$ and $I^-(H_2O)_{1-4}$.

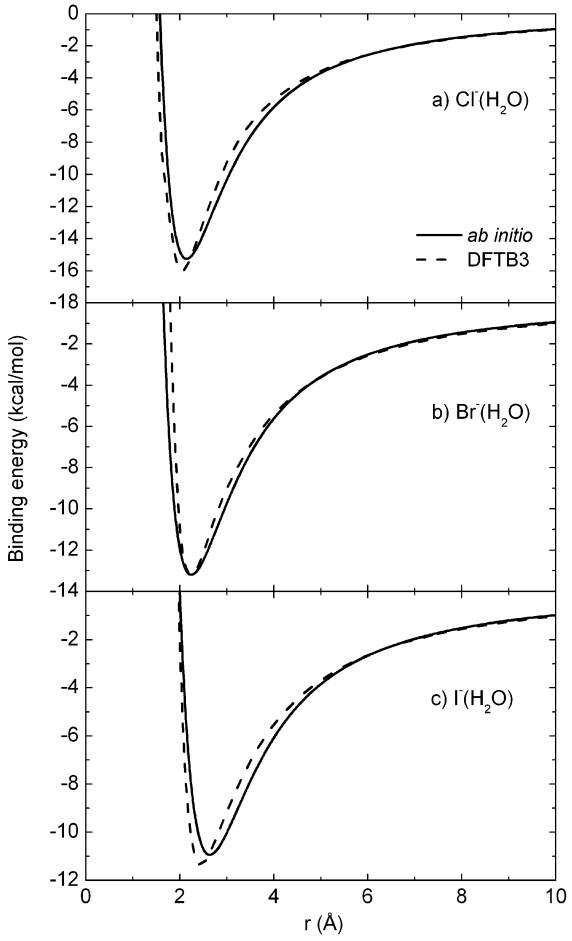

Figure 5. Potential energy curves for X^-−water interactions (X = Cl, Br, I): ab initio = MP2/aug-cc-pVTZ for $Cl^-(H_2O)$ and MP2/aug-cc-pVTZ-PP for $Br^-(H_2O)$ and $I^-(H_2O)$. The horizontal axis coordinate is the hydrogen bond distance between each halide anion and water.

cannot be unequivocally identified. However, approximate assignment of the vibrational modes reveals similar deviations to those observed for the smaller clusters. In fact, DFTB3 vibrational frequencies correlate well with their ab initio counterparts, as shown in Figure 6. Overall, DFTB3 values for low and very high frequencies are in good agreement with ab initio ones, while intermediate frequencies are systematically underestimated.

3.2.2. Bromide−Water Clusters. As in the case of chloride−water clusters, DFTB3 is found to underestimate bond lengths and angles in $Br^-(H_2O)_{1-4}$ relative to DFT and ab initio values (cf. Table 5). DFTB3 hydrogen-bond lengths are in better agreement with ab initio values, with average deviations of about 0.016 Å, whereas the average deviation reaches 0.12 Å for DFT data. On the other hand, the DFTB3 bond angles are closer to DFT values, within 6°, whereas the average deviation from ab initio data is 10°.

As was observed for chloride−water clusters, DFTB3 predicts accurate stepwise binding energies relative to DFT and ab initio values, and the average deviations are about 0.8 and 0.3 kcal/mol, respectively (cf. Figure 4). The DFTB3 results parallel their ab initio counterparts, presumably due to the better agreement of bond lengths as mentioned earlier for chloride−water clusters. Without addition of the modified γ^h function and third-order correction to the DFTB2 model, the

dx.doi.org/10.1021/ct300919h | J. Chem. Theory Comput. 2013, 9, 3321−3332

Table 7. Vibrational Frequencies of $X^-(H_2O)_{1,2}$ (X = Cl, Br, I) Clusters[a]

	$Cl^-(H_2O)$				$Br^-(H_2O)$				$I^-(H_2O)$			
	DFTB3	DFT[b]	ab initio[c]	exp[d]	DFTB3	DFT[b]	ab initio[c]	exp[d]	DFTB3	DFT[b]	ab initio[c]	exp[d]
1 (ν_{OX})[e]	229	197	203	210/232	185	163	170	158/165	149	133	143	121/131
2 (ν_{ip})[e]	311	352	369	309	284	317	337	223/275	224	268	277	160/251
3 (ν_{oop})[e]	738	737	755	738	655	664	704	664	595	589	625	
4 (ν_{HOH})[e]	1427	1688	1670	1653	1433	1682	1663	1647	1441	1675	1655	1639
5 (ν_{OHi})[e]	2922	3339	3335	3146	3161	3446	3426	3296	3337	3552	3526	3393/3422
6 (ν_{OHf})[e]	3767	3848	3891	3697	3777	3847	3891	3695	3787	3845	3889	3692/3706
Δ_{abs} (exp)[f]	88	75	83		83	68	80		80	79	83	
Δ (exp)[g]	5	6	7		8	7	10		9	9	12	
	$Cl^-(H_2O)_2$				$Br^-(H_2O)_2$				$I^-(H_2O)_2$			
	DFTB3	DFT[b]	ab initio[c]	exp[h]	DFTB3	DFT[b]	ab initio[c]	exp[h]	DFTB3	DFT[b]	ab initio[c]	exp[h]
1	110	104	101		97	90	97		69	78	90	
2	162	140	152		158	143	152		150	131	145	
3	217	190	178		197	186	177		178	167	162	
4	244	213	216		219	181	183		212	189	182	
5	314	351	356		294	320	334		221	269	294	
6	375	430	411		378	411	402		353	394	388	
7	410	511	469		405	484	473		380	439	460	
8	655	688	675		620	666	767		595	660	706	
9	772	822	810		700	766	651		654	694	622	
10	1407	1675	1661		1412	1669	1655		1413	1662	1648	
11	1452	1715	1695		1449	1709	1690		1443	1703	1685	
12 (ν_{OHi})[e]	2890	3307	3314	3130	3085	3388	3386	3207	3208	3478	3467	3331
13 (ν_{OHi})[e]	3370	3584	3588	3375	3409	3643	3625	3438	3459	3689	3674	3500
14 (ν_{OHw})[e]	3655	3750	3796	3633	3678	3735	3789	3625	3714	3731	3778	3616
15 (ν_{OHf})[e]	3761	3841	3885	3686	3768	3838	3881	3680	3773	3834	3876	3675
Δ_{abs} (exp)	86	165	190		73	164	183		90	153	168	
Δ (exp)	3	5	6		2	5	5		3	4	5	

[a]All calculated values are harmonic vibrational frequencies. All frequencies are in inverse centimeters. [b]B3LYP/cc-pVTZ for $Cl^-(H_2O)_{1,2}$ and B3LYP/cc-pVTZ-PP for $Br^-(H_2O)_{1-2}$ and $I^-(H_2O)_{1,2}$. [c]MP2/aug-cc-pVTZ for $Cl^-(H_2O)_{1,2}$ and MP2/aug-cc-pVTZ-PP for $Br^-(H_2O)_{1-2}$ and $I^-(H_2O)_{1,2}$. [d]From ref 73. [e]OX = halide-water stretch; ip = in-plane bend; oop = out-of-plane bend; HOH = water bend; OHi = ion-hydrogen-bonded OH stretch; OHw = water-hydrogen-bonded O−H stretch; OHf = free O−H stretch. [f]Average absolute deviation from reference data in parentheses (cm^{-1}). [g]Average absolute deviation from reference data in parentheses (%). [h]From ref 74.

calculated binding energies deviate from ab initio data by about 3 kcal/mol. As shown from the data in Table 8, the accuracy of the predicted atomic partial charges is improved by including the hydrogen bond and third-order corrections in the DFTB3 model, although the uncorrected DFTB2 predicts partial charges in qualitative agreement with reference data. Moreover, as shown in Figure 5b, the DFTB3 potential energy curve for the bromide−water binary cluster is in perfect agreement with its ab initio counterpart.

DFTB3 underestimates the stretching frequency of the O−H bond implicated in hydrogen bonding to the ion in $Br^-(H_2O)_1$ relative to DFT and experimental values, but it overestimates the magnitude of its red shift upon hydrogen bonding by 215 and 217 cm^{-1}, respectively (cf. Table 7). The average deviation of the DFTB3 frequencies from their experimental counterparts is similar to that predicted by DFT and ab initio quantum chemistry and comparable to that observed for chloride, but it is larger than that from DFT data. Similar trends as those discussed for chloride−water are observed for larger clusters as well. In general, DFTB3 frequencies correlate well with their ab initio counterparts, as shown in Figure 6.

3.2.3. Iodide−Water Clusters. Inspection of Table 6 reveals that the DFTB3 bond lengths in $I^-(H_2O)_{1-4}$ are smaller than their DFT and ab initio counterparts by about 0.196 and 0.046 Å, respectively, whereas bond angles are found in better agreement with DFT values (average deviation of less than 6°) than with ab initio values (average deviation of about 12°). These results are comparable to those observed previously for the other halides.

Like for the other halides, DFTB3 stepwise binding energies are in quantitative agreement with DFT and ab initio values, with deviations about 0.7 and 0.2 kcal/mol, respectively. Inclusion of hydrogen-bond and third-order corrections in DFTB3 improves the binding energies by about 2 kcal/mol compared to DFTB2 results. As shown from the data in Table 8, DFTB atomic partial charges are systematically improved upon inclusion of such corrections, similarly to what was observed in previous systems. It is important to note that, the minimal basis set approach of DFTB, which might cause the model to underestimate the polarizability of iodide, does not have a very significant effect on cluster binding energies in the first place, and inclusion of hydrogen bond and third-order corrections partly compensate for this potential shortcoming as they predict accurate charge distributions. As for the other halides, the DFTB3 iodide−water potential energy curve, shown in Figure 5c, is in good agreement with its ab initio counterpart.

For $I^-(H_2O)_1$, the DFTB3 frequencies are underestimated relative to DFT and ab initio values in most cases and they are found in better agreement with experimental data (cf. Table 7). The magnitude of the red shift of the stretching frequency of the O−H bond implicated in hydrogen bonding with the ion is

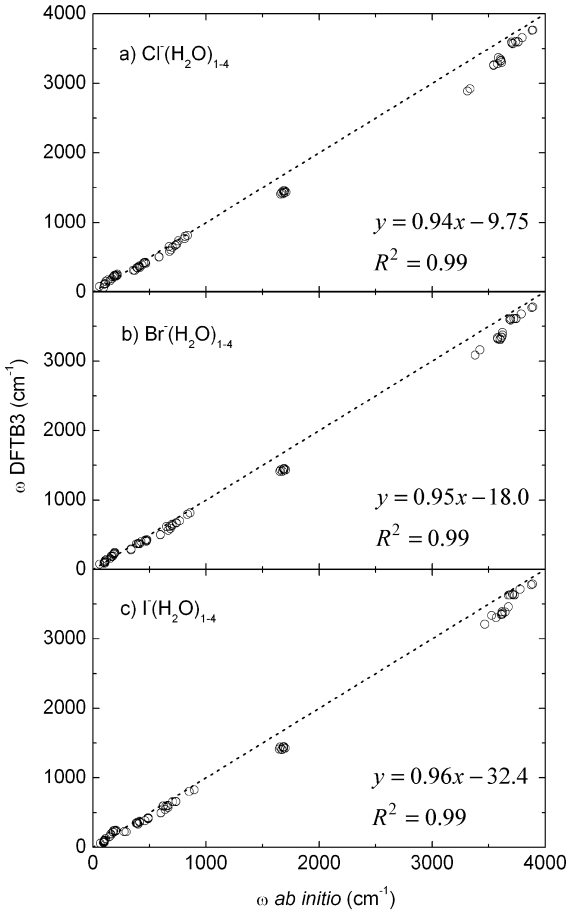

Figure 6. Calculated harmonic vibrational frequencies for $X^-(H_2O)_{1-4}$ clusters (X = Cl, Br, I): ab initio = MP2/aug-cc-pVTZ for $Cl^-(H_2O)_1$ and MP2/aug-cc-pVTZ-PP for $Br^-(H_2O)_1$ and $I^-(H_2O)_1$.

Table 8. Atomic Partial Charge Distributions in $X^-(H_2O)$ Clusters (X = Cl, Br, I)

cluster	atom	DFTB2	DFTB3	ESP[a]
$Cl^-(H_2O)$	Cl	−0.9478	−0.9488	−0.9332
	H	0.3413	0.4238	0.4459
	O	−0.6692	−0.8301	−0.8539
	H	0.2757	0.3551	0.3412
Δ[b]		16.5	3.4	
$Br^-(H_2O)$	Br	−0.9597	−0.9660	−0.9443
	H	0.3370	0.4158	0.4277
	O	−0.6580	−0.8070	−0.8289
	H	0.2806	0.3572	0.3456
Δ		15.6	2.8	
$I^-(H_2O)$	I	−0.9803	−0.9785	−0.9394
	H	0.3330	0.4076	0.4142
	O	−0.6416	−0.7906	−0.8184
	H	0.2889	0.3615	0.3437
Δ		15.4	3.6	

[a]Atomic partial charges obtained from the electrostatic surface potential (ESP)[75−77] with MP2/aug-cc-pVTZ for $Cl^-(H_2O)$ and MP2/aug-cc-pVTZ-PP for $Br^-(H_2O)$ and $I^-(H_2O)$. [b]Δ is the absolute mean deviation from ESP data (%).

smaller than for chloride and bromide, presumably due to the weaker iodide−water interaction. Moreover, the average deviation of the DFTB3 frequencies from experimental data is comparable to that predicted by DFT and ab initio quantum chemistry and it is comparable to those of other halides. The deviations of DFTB3 frequencies from their experimental counterparts for larger clusters are comparable to that of the other halides, but DFTB3 seems to perform slightly better for iodide−water clusters than for chloride−water and bromide−water clusters. In general, DFTB3 frequencies correlate well with their ab initio counterparts, as shown in Figure 6.

4. CONCLUSIONS

New parameter sets have been developed to describe the interactions between halogen atoms and oxygen and hydrogen atoms by the approximate DFT-based DFTB3 model. The parameters have been used to investigate the main structural, energetic, and vibrational properties of various halogen-containing molecules as well as halide−water clusters. The newly parametrized DFTB3 model predicts acceptable structural properties, atomization energies, and vibrational frequencies for small halogen-containing molecules, in good agreement with reference DFT data, but deviations increase for larger molecules containing multiple halide−oxygen double bonds. More importantly for the purpose at hand, the model accurately predicts the structures, energetics, and vibrational frequencies of halide−water clusters, when compared to the results of high-level MP2/aug-cc-pVTZ calculations and to available experimental data. Overall, hydrogen bond lengths and angles are slightly underestimated by DFTB3, but binding energies are in quantitative agreement with ab initio data (within less than 0.5 kcal/mol), excellent agreement due to inclusion of hydrogen-bond and third-order corrections in this model. The model also predicts vibrational frequencies in good qualitative agreement with ab initio and experimental data. The relative accuracy of DFTB3 in predicting solvation properties of ions, together with its computational efficiency, make it a promising model for investigating much larger clusters and describing interatomic interactions in molecular dynamics simulations of such systems.

■ ASSOCIATED CONTENT

Supporting Information

Atomic spin constants for chlorine, bromine, and iodine atoms. Vibrational frequencies of molecules investigated. This material is available free of charge via the Internet at http://pubs.acs.org.

■ AUTHOR INFORMATION

Corresponding Author

*E-mail: Gilles.Peslherbe@Concordia.Ca.

Notes

The authors declare no competing financial interest.

■ ACKNOWLEDGMENTS

The authors would like to thank Prof. Marcus Elstner and Dr. Michael Gaus for fruitful discussions and anonymous reviewers for insightful comments. Financial support for this work has been provided by the Natural Sciences and Engineering Research Council of Canada (NSERC) and the Bremen Center for Computational Materials Science (BCCMS). Calculations were performed at the Centre for Research in Molecular Modeling (CERMM) and Calcul Québec. G.H.P. is the recipient of a Concordia University Research Chair, and S.J. is the recipient of a Concordia University Fellowship.

REFERENCES

(1) Meot-Ner, M. The Ionic Hydrogen Bond. *Chem. Rev.* **2005**, *105*, 213−284.
(2) Jungwirth, P.; Tobias, D. J. Specific Ion Effects at the Air/Water Interface. *Chem. Rev.* **2006**, *106*, 1259−1281.
(3) Chang, T.-M.; Dang, L. X. Recent Advances in Molecular Simulations of Ion Solvation at Liquid Interfaces. *Chem. Rev.* **2006**, *106*, 1305−1322.
(4) Marcus, Y. Effect of Ions on the Structure of Water: Structure Making and Breaking. *Chem. Rev.* **2009**, *109*, 1346−1370.
(5) Netz, R. R.; Horinek, D. Progress in Modeling of Ion Effects at the Vapor/Water Interface. *Annu. Rev. Phys. Chem.* **2012**, *63*, 401−418.
(6) Jungwirth, P.; Tobias, D. J. Molecular Structure of Salt Solutions: A New View of the Interface with Implications for Heterogeneous Atmospheric Chemistry. *J. Phys. Chem. B* **2001**, *105*, 10468−10472.
(7) Ghosal, S.; Hemminger, J. C.; Bluhm, H.; Mun, B. S.; Hebenstreit, E. L. D.; Ketteler, G.; Ogletree, D. F.; Requejo, F. G.; Salmeron, M. Electron Spectroscopy of Aqueous Solution Interfaces Reveals Surface Enhancement of Halides. *Science* **2005**, *307*, 563−566.
(8) Levin, Y. Polarizable Ions at Interfaces. *Phys. Rev. Lett.* **2009**, *102*, 147803.
(9) Caleman, C.; Hub, J. S.; van Maaren, P. J.; van der Spoel, D. Atomistic Simulation of Ion Solvation in Water Explains Surface Preference of Halides. *Proc. Natl. Acad. Sci. U.S.A.* **2011**, *108*, 6838−6842.
(10) Baer, M. D.; Mundy, C. J. Toward an Understanding of the Specific Ion Effect Using Density Functional Theory. *J. Phys. Chem. Lett.* **2011**, *2*, 1088−1093.
(11) Cacace, M. G.; Landau, E. M.; Ramsden, J. J. The Hofmeister Series: Salt and Solvent Effects on Interfacial Phenomena. *Q. Rev. Biophys.* **1997**, *30*, 241−277.
(12) Tobias, D. J.; Hemminger, J. C. Getting Specific about Specific Ion Effects. *Science* **2008**, *319*, 1197−1198.
(13) Koch, D. M.; Peslherbe, G. H. On the Transition from Surface to Interior Solvation in Iodide−Water Clusters. *Chem. Phys. Lett.* **2002**, *359*, 381−389.
(14) Nguyen, T.-N. V.; Hughes, S. R.; Peslherbe, G. H. Microsolvation of the Sodium and Iodide Ions and Their Ion Pair in Acetonitrile Clusters: A Theoretical Study. *J. Phys. Chem. B* **2008**, *112*, 621−635.
(15) Hernández de la Peña, L.; Peslherbe, G. H. Quantum Effects on the Free Energy of Ionic Aqueous Clusters Evaluated by Nonequilibrium Computational Methods. *J. Phys. Chem. B* **2010**, *114*, 5404−5411.
(16) Dang, L. X.; Rice, J. E.; Caldwell, J.; Kollman, P. A. Ion Solvation in Polarizable Water: Molecular Dynamics Simulations. *J. Am. Chem. Soc.* **1991**, *113*, 2481−2486.
(17) Dang, L. X.; Garrett, B. C. Photoelectron Spectra of the Hydrated Iodine Anion from Molecular Dynamics Simulations. *J. Chem. Phys.* **1993**, *99*, 2972−2977.
(18) Perera, L.; Berkowitz, M. L. Many-Body Effects in Molecular Dynamics Simulations of $Na^+(H_2O)_n$ and $Cl^-(H_2O)_n$ Clusters. *J. Chem. Phys.* **1991**, *95*, 1954−1963.
(19) Sremaniak, L. S.; Perera, L.; Berkowitz, M. L. Enthalpies of Formation and Stabilization Energies of $Br^-(H_2O)_n$ (n = 1, 2, ..., 15) Clusters. Comparisons between Molecular Dynamics Computer Simulations and Experiment. *Chem. Phys. Lett.* **1994**, *218*, 377−382.
(20) Vazdar, M.; Pluharova, E.; Mason, P. E.; Vacha, R.; Jungwirth, P. Ions at Hydrophobic Aqueous Interfaces: Molecular Dynamics with Effective Polarization. *J. Phys. Chem. Lett.* **2012**, *3*, 2087−2091.
(21) Porezag, D.; Frauenheim, T.; Köhler, T.; Seifert, G.; Kaschner, R. Construction of Tight-Binding-Like Potentials on the Basis of Density-Functional Theory: Application to Carbon. *Phys. Rev. B* **1995**, *51*, 12947−12957.
(22) Elstner, M.; Frauenheim, T.; Suhai, S. An Approximate DFT Method for QM/MM Simulations of Biological Structures and Processes. *J. Mol. Struct. (THEOCHEM)* **2003**, *632*, 29−41.
(23) Elstner, M.; Porezag, D.; Jungnickel, G.; Elsner, J.; Haugk, M.; Frauenheim, T.; Suhai, S.; Seifert, G. Self-Consistent-Charge Density-Functional Tight-Binding Method for Simulations of Complex Materials Properties. *Phys. Rev. B* **1998**, *58*, 7260−7268.
(24) Frauenheim, T.; Seifert, G.; Elstner, M.; Hajnal, Z.; Jungnickel, G.; Porezag, D.; Suhai, S.; Scholz, R. A Self-Consistent Charge Density-Functional Based Tight-Binding Method for Predictive Materials Simulations in Physics, Chemistry and Biology. *Phys. Status Solidi B-Basic Res.* **2000**, *217*, 41−62.
(25) Frauenheim, T.; Seifert, G.; Elstner, M.; Niehaus, T.; Köhler, C.; Amkreutz, M.; Sternberg, M.; Hajnal, Z.; Di Carlo, A.; Suhai, S. Atomistic Simulations of Complex Materials: Ground-State and Excited-State Properties. *J. Phys.: Condens. Matter* **2002**, *14*, 3015−3047.
(26) Witek, H. A.; Morokuma, K. Systematic Study of Vibrational Frequencies Calculated with the Self-Consistent Charge Density Functional Tight-Binding Method. *J. Comput. Chem.* **2004**, *25*, 1858−1864.
(27) Hazebroucq, S.; Picard, G. S.; Adamo, C.; Heine, T.; Gemming, S.; Seifert, G. Density-Functional-Based Molecular-Dynamics Simulations of Molten Salts. *J. Chem. Phys.* **2005**, *123*, 134510.
(28) Zheng, G.; Irle, S.; Morokuma, K. Performance of the DFTB Method in Comparison to DFT and Semiempirical Methods for Geometries and Energies of C_{20}−C_{86} Fullerene Isomers. *Chem. Phys. Lett.* **2005**, *412*, 210−216.
(29) Kruger, T.; Elstner, M.; Schiffels, P.; Frauenheim, T. Validation of the Density-Functional Based Tight-Binding Approximation Method for the Calculation of Reaction Energies and Other Data. *J. Chem. Phys.* **2005**, *122*, 114110.
(30) Köhler, C.; Frauenheim, T. Molecular Dynamics Simulations of CF_x (x = 2, 3) Molecules at Si_3N_4 and SiO_2 Surfaces. *Surf. Sci.* **2006**, *600*, 453−460.
(31) Choi, T. H.; Jordan, K. D. Application of the SCC-DFTB Method to $H^+(H_2O)_6$, $H^+(H_2O)_{21}$, and $H^+(H_2O)_{22}$. *J. Phys. Chem. B* **2010**, *114*, 6932−6936.
(32) Goyal, P.; Elstner, M.; Cui, Q. Application of the SCC-DFTB Method to Neutral and Protonated Water Clusters and Bulk Water. *J. Phys. Chem. B* **2011**, *115*, 6790−6805.
(33) Gaus, M.; Cui, Q.; Elstner, M. DFTB3: Extension of the Self-Consistent-Charge Density-Functional Tight-Binding Method (SCC-DFTB). *J. Chem. Theory Comput.* **2011**, *7*, 931−948.
(34) Gaus, M.; Goez, A.; Elstner, M. Parametrization and Benchmark of DFTB3 for Organic Molecules. *J. Chem. Theory Comput.* **2013**, *9*, 338−354.
(35) Yang, Y.; Yu, H.; York, D.; Elstner, M.; Cui, Q. Description of Phosphate Hydrolysis Reactions with the Self-Consistent-Charge Density-Functional-Tight-Binding (SCC-DFTB) Theory. 1. Parameterization. *J. Chem. Theory Comput.* **2008**, *4*, 2067−2084.
(36) Moreira, N. H.; Dolgonos, G.; Aradi, B.; da Rosa, A. L.; Frauenheim, T. Toward an Accurate Density-Functional Tight-Binding Description of Zinc-Containing Compounds. *J. Chem. Theory Comput.* **2009**, *5*, 605−614.
(37) Dolgonos, G.; Aradi, B.; Moreira, N. H.; Frauenheim, T. An Improved Self-Consistent-Charge Density-Functional Tight-Binding (SCC-DFTB) Set of Parameters for Simulation of Bulk and Molecular Systems Involving Titanium. *J. Chem. Theory Comput.* **2010**, *6*, 266−278.
(38) Sarkar, S.; Pal, S.; Sarkar, P.; Rosa, A. L.; Frauenheim, T. Self-Consistent-Charge Density-Functional Tight-Binding Parameters for Cd−X (X = S, Se, Te) Compounds and Their Interaction with H, O, C, and N. *J. Chem. Theory Comput.* **2011**, *7*, 2262−2276.
(39) Grundkötter-Stock, B.; Bezugly, V.; Kunstmann, J.; Cuniberti, G.; Frauenheim, T.; Niehaus, T. A. SCC-DFTB Parametrization for Boron and Boranes. *J. Chem. Theory Comput.* **2012**, *8*, 1153−1163.
(40) Elstner, M. The SCC-DFTB Method and Its Application to Biological Systems. *Theor. Chem. Acc.* **2006**, *116*, 316−325.
(41) Slater, J. C.; Koster, G. F. Simplified LCAO Method for the Periodic Potential Problem. *Phys. Rev.* **1954**, *94*, 1498−1524.
(42) The data is usually fitted by an appropriate analytical (usually, polynomial) function which is further represented in the form of cubic splines for a given range of interatomic distances. Alternatively, one

can use a mixed exponential−Gaussian function of the form $E_{rep}(r) = A\exp(-Br) + C\exp(-Dr^2)$ that only requires four parameters (A, B, C, D) to be fitted, unlike high-order polynomials [Dolgonos, G. unpublished work]. The latter function is commonly used successfully for complete-basis-set (CBS) extrapolations [Peterson, K. A.; Woon, D. E.; Dunning, T. H. *J. Chem. Phys.* **1994**, *100*, 7410−7415]. The mixed exponential−Gaussian function fit of the repulsion curves was found to produce improved vibrational frequencies for halogen-containing molecules.

(43) Elstner, M. SCC-DFTB: What Is the Proper Degree of Self-Consistency? *J. Phys. Chem. A* **2007**, *111*, 5614−5621.

(44) Yang, Y.; Yu, H.; York, D.; Cui, Q.; Elstner, M. Extension of the Self-Consistent-Charge Density-Functional Tight-Binding Method: Third-Order Expansion of the Density Functional Theory Total Energy and Introduction of a Modified Effective Coulomb Interaction. *J. Phys. Chem. A* **2007**, *111*, 10861−10873.

(45) Perdew, J. P.; Burke, K.; Ernzerhof, M. Generalized Gradient Approximation Made Simple. *Phys. Rev. Lett.* **1996**, *77*, 3865−3868.

(46) Adamo, C.; Barone, V. Toward Reliable Density Functional Methods without Adjustable Parameters: The PBE0 Model. *J. Chem. Phys.* **1999**, *110*, 6158−6170.

(47) Stephens, P. J.; Devlin, F. J.; Chabalowski, C. F.; Frisch, M. J. Ab Initio Calculation of Vibrational Absorption and Circular Dichroism Spectra Using Density Functional Force Fields. *J. Phys. Chem.* **1994**, *98*, 11623−11627.

(48) Becke, A. D. Density-Functional Thermochemistry. III. The Role of Exact Exchange. *J. Chem. Phys.* **1993**, *98*, 5648−5652.

(49) Lee, C.; Yang, W.; Parr, R. G. Development of the Colle-Salvetti Correlation-Energy Formula into a Functional of the Electron Density. *Phys. Rev. B* **1988**, *37*, 785−789.

(50) Francl, M. M.; Pietro, W. J.; Hehre, W. J.; Binkley, J. S.; Gordon, M. S.; DeFrees, D. J.; Pople, J. A. Self-Consistent Molecular Orbital Methods. XXIII. A Polarization-Type Basis Set for Second-Row Elements. *J. Chem. Phys.* **1982**, *77*, 3654−3665.

(51) Rassolov, V. A.; Ratner, M. A.; Pople, J. A.; Redfern, P. C.; Curtiss, L. A. 6-31G* Basis Set for Third-Row Atoms. *J. Comput. Chem.* **2001**, *22*, 976−984.

(52) Glukhovtsev, M. N.; Pross, A.; McGrath, M. P.; Radom, L. Extension of Gaussian-2 (G2) Theory to Bromine- and Iodine-Containing Molecules: Use of Effective Core Potentials. *J. Chem. Phys.* **1995**, *103*, 1878−1885.

(53) Feller, D. The Role of Databases in Support of Computational Chemistry Calculations. *J. Comput. Chem.* **1996**, *17*, 1571−1586.

(54) Schuchardt, K. L.; Didier, B. T.; Elsethagen, T.; Sun, L.; Gurumoorthi, V.; Chase, J.; Li, J.; Windus, T. L. Basis Set Exchange: A Community Database for Computational Sciences. *J. Chem. Inf. Model.* **2007**, *47*, 1045−1052.

(55) Woon, D. E.; Dunning, T. H. Gaussian Basis Sets for Use in Correlated Molecular Calculations. III. The Atoms Aluminum through Argon. *J. Chem. Phys.* **1993**, *98*, 1358−1371.

(56) Peterson, K. A.; Figgen, D.; Goll, E.; Stoll, H.; Dolg, M. Systematically Convergent Basis Sets with Relativistic Pseudopotentials. II. Small-Core Pseudopotentials and Correlation Consistent Basis Sets for the Post-d Group 16−18 Elements. *J. Chem. Phys.* **2003**, *119*, 11113−11123.

(57) Peterson, K. A.; Shepler, B. C.; Figgen, D.; Stoll, H. On the Spectroscopic and Thermochemical Properties of ClO, BrO, IO, and Their Anions. *J. Phys. Chem. A* **2006**, *110*, 13877−13883.

(58) Lee, H. M.; Kim, K. S. Structures and Spectra of Iodide−Water Clusters $I^-(H_2O)_{n=1-6}$: An Ab Initio Study. *J. Chem. Phys.* **2001**, *114*, 4461−4471.

(59) Masamura, M. Structures, Energetics, and Spectra of $Br^-(H_2O)_n$ clusters, n = 1−6: Ab Initio Study. *J. Chem. Phys.* **2003**, *118*, 6336−6347.

(60) Aradi, B.; Hourahine, B.; Frauenheim, T. DFTB+, a Sparse Matrix-based Implementation of the DFTB Method. *J. Phys. Chem. A* **2007**, *111*, 5678−5684.

(61) Frisch, M. J.; Trucks, G. W.; Schlegel, H. B.; Scuseria, G. E.; Robb, M. A.; Cheeseman, J. R.; Scalmani, G.; Barone, V.; Mennucci, B.; Petersson, G. A.; Nakatsuji, H.; Caricato, M.; Li, X.; Hratchian, H. P.; Izmaylov, A. F.; Bloino, J.; Zheng, G.; Sonnenberg, J. L.; Hada, M.; Ehara, M.; Toyota, K.; Fukuda, R.; Hasegawa, J.; Ishida, M.; Nakajima, T.; Honda, Y.; Kitao, O.; Nakai, H.; Vreven, T.; Montgomery, Jr., J. A.; Peralta, J. E.; Ogliaro, F.; Bearpark, M.; Heyd, J. J.; Brothers, E.; Kudin, K. N.; Staroverov, V. N.; Kobayashi, R.; Normand, J.; Raghavachari, K.; Rendell, A.; Burant, J. C.; Iyengar, S. S.; Tomasi, J.; Cossi, M.; Rega, N.; Millam, J. M.; Klene, M.; Knox, J. E.; Cross, J. B.; Bakken, V.; Adamo, C.; Jaramillo, J.; Gomperts, R.; Stratmann, R. E.; Yazyev, O.; Austin, A. J.; Cammi, R.; Pomelli, C.; Ochterski, J. W.; Martin, R. L.; Morokuma, K.; Zakrzewski, V. G.; Voth, G. A.; Salvador, P.; Dannenberg, J. J.; Dapprich, S.; Daniels, A. D.; Farkas, Ö.; Foresman, J. B.; Ortiz, J. V.; Cioslowski, J.; Fox, D. J. *Gaussian 09*, Revision B.01; Gaussian, Inc.: Wallingford CT, 2009.

(62) Köhler, C.; Frauenheim, T.; Hourahine, B.; Seifert, G.; Sternberg, M. Treatment of Collinear and Noncollinear Electron Spin within an Approximate Density Functional Based Method. *J. Phys. Chem. A* **2007**, *111*, 5622−5629.

(63) Møller, C.; Plesset, M. S. Note on an Approximation Treatment for Many-Electron Systems. *Phys. Rev.* **1934**, *46*, 618−622.

(64) Boys, S. F.; Bernardi, F. The Calculation of Small Molecular Interactions by the Differences of Separate Total Energies. Some Procedures with Reduced Errors. *Mol. Phys.* **1970**, *19*, 553−566.

(65) Jahangiri, S.; Peslherbe, G. H. Unpublished work.

(66) Roscioli, J. R.; Diken, E. G.; Johnson, M. A.; Horvath, S.; McCoy, A. B. Prying Apart a Water Molecule with Anionic H-Bonding: A Comparative Spectroscopic Study of the $X^-\cdot H_2O$ (X = OH, O, F, Cl, and Br) Binary Complexes in the 600−3800 cm^{-1} Region. *J. Phys. Chem. A* **2006**, *110*, 4943−4952.

(67) Huber, K. P.; Herzberg, G. *Molecular Spectra and Molecular Structure. IV. Constants of Diatomic Molecules*; Van Nostrand Reinhold Company: New York, 1979.

(68) Deeley, C. M.; Mills, I. M. Vibration-Rotation Spectra and the Harmonic Force Field of HOCl. *J. Mol. Spectrosc.* **1985**, *114*, 368−376.

(69) Casper, B.; Mack, H.-G.; Muller, H. S. P.; Willner, H.; Oberhammer, H. Molecular Structures of Perchloric Acid and Halogen Perchlorates $ClOClO_3$ and $FOClO_3$. *J. Phys. Chem.* **1994**, *98*, 8339−8342.

(70) Linstrom, P. J.; Mallard, W. G. *NIST Chemistry WebBook, NIST Standard Reference Database Number 69*; National Institute of Standards and Technology, http://webbook.nist.gov (retrieved October 2012).

(71) Koga, Y.; Takeo, H.; Kondo, S.; Sugie, M.; Matsumura, C.; McRae, G. A.; Cohen, E. A. The Rotational Spectra, Molecular Structure, Dipole Moment, and Hyperfine Constants of HOBr and DOBr. *J. Mol. Spectrosc.* **1989**, *138*, 467−481.

(72) Ozeki, H.; Saito, S. Submillimeter-Wave Spectra of Hypoiodous Acid. *J. Chem. Phys.* **2004**, *120*, 5110−5116.

(73) Horvath, S.; McCoy, A. B.; Elliott, B. M.; Weddle, G. H.; Roscioli, J. R.; Johnson, M. A. Anharmonicities and Isotopic Effects in the Vibrational Spectra of $X^-\cdot H_2O$, $\cdot HDO$, and $\cdot D_2O$ [X = Cl, Br, and I] Binary Complexes. *J. Phys. Chem. A* **2010**, *114*, 1556−1568.

(74) Ayotte, P.; Nielsen, S. B.; Weddle, G. H.; Johnson, M. A.; Xantheas, S. S. Spectroscopic Observation of Ion-Induced Water Dimer Dissociation in the $X^-\cdot(H_2O)_2$ (X = F, Cl, Br, I) Clusters. *J. Phys. Chem. A* **1999**, *103*, 10665−10669.

(75) Singh, U. C.; Kollman, P. A. An Approach to Computing Electrostatic Charges for Molecules. *J. Comput. Chem.* **1984**, *5*, 129−145.

(76) Besler, B. H.; Merz, K. M.; Kollman, P. A. Atomic Charges Derived from Semiempirical Methods. *J. Comput. Chem.* **1990**, *11*, 431−439.

(77) Hu, H.; Lu, Z.; Yang, W. Fitting Molecular Electrostatic Potentials from Quantum Mechanical Calculations. *J. Chem. Theory Comput.* **2007**, *3*, 1004−1013.